

# Journal of Mechanics of Materials and Structures

**CIRCULAR-HOLE STRESS CONCENTRATION ANALYSIS ON  
GLASS-FIBER-COTTON REINFORCED MC-NYLON**

You Rui Tao, Ning Rui Li and Xu Han

**Volume 13, No. 3**

**May 2018**





## CIRCULAR-HOLE STRESS CONCENTRATION ANALYSIS ON GLASS-FIBER-COTTON REINFORCED MC-NYLON

YOU RUI TAO, NING RUI LI AND XU HAN

The influence of geometrical discontinuities on the stress distribution is critical for design applications. A novel type of composite, named glass-fiber-cotton reinforced monomer casting nylon (GFCR MC-nylon), is prepared, and the circular-hole stress concentration of a GFCR MC-nylon plate is investigated via the digital image correlation technique (DIC). The experimental results show that the stress concentration factor (SCF) of the composite varies with the diameter of the circular hole and stress intensity. A novel finite element model is established to investigate the influence of glass-fiber (GF) length on SCF. The simulation results show high agreement with the experimental results. The findings provide the basis for the structure design of fiber-cotton reinforced composite.

### 1. Introduction

For a homogeneous thin panel with a circular hole subjected to uniaxial loading, the distribution of stress is not monotonic around the circular hole. The stress concentration factor (SCF) is defined as the stress around the circular hole divided by the average stress. Generally, the maximum SCF is located at the hole edge.

Nowadays, fiber-reinforced composites have been widely applied in industry. The stress concentration of fiber-reinforced composites has attracted attention in the recent past. If the fiber under consideration is an isotropic material with a circular hole, Cheng and Chen [1988] have provided equations to solve the SCF for plane-stress analysis. The equations show that the distribution of stress is determined by the proportion and elastic modulus of the fiber and resin. Maximyuk et al. [2014] studied the nonlinear deformation of flexible composite shells with a reinforced curved hole under static loading. Pandita and Nishiyabu [Pandita et al. 2003] investigated the tensile strain field of woven fabric composites with digital photogrammetry technology. The experimental results revealed the strain concentrations near the singularity and that the strain concentrations were influenced by the tensile loading direction and the hole dimension relative to the size of the unit cell of the plain woven fabrics. Ghasemi and Razavian [2012] advocated that the influence of specimen dimension, notch size, lay ups, and material properties were important to the residual strength and stress concentration factor of laminated composite materials. Defense hole systems are used to redistribute the stresses around the main hole by introducing an auxiliary hole in the low-stress area near the main hole. Jadee and Othman [2015] investigated the effect of the defense hole system on the stress distribution around the bolt-hole in a GF reinforced polymer composite bolted joint, showing that adding an auxiliary hole near the bolt-hole reduces the stresses in the vicinity of the bolt hole. Toubal et al. [2005] investigated the stress concentration characterization of a laminate carbon epoxy with an electronic speckle pattern interferometer, which were compared with the predictions of a

*Keywords:* concentration, fiber-reinforced composite, digital image correlation technique, simulation.

theoretical model previously developed by Lekhnitskii [Lekhnitskii et al. 1968] and a finite element study. Liu and Huang [2014] thought that the SCF with transversely isotropic fibers involved can be sufficiently approximated by a much simpler stress concentration factor formula derived upon isotropic fiber reinforcement. Liu and Tang [2016] studied the stress concentration in notched cross-ply laminates under tensile loading. Some other researchers focused on the influence of ply cluster thickness and location on matrix cracking evolution in open-hole composite laminates [Moure et al. 2016], progressive failure analysis on scaled open-hole tensile composite laminates [Bao and Liu 2016], gradient model [Khoroshun and Kabysch 2007], and a unified approach to problems of stress concentration near V-shaped notches [Savruk and Kazberuk 2007]. The above references show that reduced stress concentration in composites has been studied widely and applied in engineering. However, there are few studies or experiments available in the literature that explain the stress concentration of long GF cotton reinforced composites.

Finite element simulation has been adopted in the stress concentration analysis of composites. For example, Wu and Mu [2003] compared the SCF in isotropic and orthotropic finite-width panels by performing systematic finite element simulations. Finite element modeling also has been applied in the stress-analysis of laminated composite plates containing circular holes under transverse loading [Paul and Rao 1995]. Hao et al. [2015] investigated the notch effects and crack propagation on kenaf/polypropylene nonwoven composites. However, the finite element modeling used in the above references was based on commercial finite element method (FEM) code, such as the Discrete Damage Mechanics model, which is not suited to analyze the influence of length and proportion of fibers on stress concentration.

New measurement technologies have been applied in the investigation of stress concentration, such as digital photogrammetry technology [Maximyuk et al. 2014], electronic speckle pattern interferometry [Toubal et al. 2005], and digital image correlation (DIC) [Aparna et al. 2015]. The DIC technique uses high-speed, high-resolution, and accurate charge-coupled device cameras for measuring displacement components on the surface of the testing material having speckle patterns. Images are captured at the time of testing at every stress cycle and these deformed patterns are correlated with a reference pattern and determining the displacements of the so-called subsets.

In this paper, the authors prepared a novel type of long GF cotton reinforced nylon through casting. The ultimate strength of the composite is more than 140 MPa. Therefore, this composite may be manufactured as a structural part in which a circular hole is always used to connect the other parts. The present study is hence aimed at investigating the stress concentration on the composite plate using the DIC technique. The arrangement of this paper is summarized as follows. The preparation of the composite and tensile samples and experimental procedure are introduced in Section 2. The experimental results of stress concentration are discussed in Section 3. Then, a novel finite element model is established and the finite element analysis results are compared with experimental results in Section 4. At last, in Section 5, the authors give the conclusions of this study.

## 2. Preparation of GFCR MC-nylon specimen

As a type of engineering plastic with high molecular weight, high mechanical advantages, and excellent self-lubricating performance, monomer casting nylon (MC-nylon) has been widely used for the production of gears, bearings, and slide blocks [Xu et al. 2013]. Many attempts have been made to improve the properties of MC-nylon [Zhang et al. 2012; Wang et al. 2013], such as incorporating GF into the plastic



resin. However, in the above researches, the mechanical properties of the composite were not improved significantly because the length of the GFs was too short.

As shown in Figure 1 (left), GF cotton is a new reinforcing material in composites. GF cotton is not a mixture of GF and cotton, but is instead gossypine long GF. In other word, GF cotton is made up nondirectional long GFs, which is loosened from a GF bundle, shown in Figure 1 (center) by a garnetting machine. In the GF bundle, the orientation of the GFs is directional. After loosening, the GF bundle is dispersed as single one. The orientation of single GF is nondirectional, as shown in Figure 1 (left). To illustrate the orientation of the GFs, a microscopic image of the fibers in a composite is shown in Figure 1 (right). It is clear that the fibers are nondirectional. In this investigation, the length of the GFs is 60 mm, which is much longer than that of short GF-reinforced composites. This novel composite is isotropic because the orientation of the GFs in the composite is nondirectional in three-dimensional space.

The raw materials in this composite include caprolactam monomer, a main catalyst, an auxiliary catalyst, and reinforced material. The caprolactam monomer was supplied by China Petroleum and Chemical Co. Sodium hydroxide (NaOH), the main catalyst, was purchased from Genert Chemical Reagent Co. (Tianjin, China). Toluene-2,4-diisocyanate (TDI), the auxiliary catalyst, was purchased from Kelong Chemical Reagent Factory (Chengdu, China). GF cotton, which acts as reinforced material, was manufactured by Nanjing GF Co. The length of monofilament of GF is 60 mm.

The preparation of the GF-cotton reinforced MC-nylon is in Figure 2. Firstly, an appropriate amount of GF cotton was put in mold preheated to 170 °C. A proper quantity of caprolactam and a small quantity of carbon powder were put into a three-necked flask, and then were heated to about 130 °C. To remove water in the caprolactam, the melting caprolactam was refluxed under vacuum for about 30 min. Then a proper amount of NaOH was added into the melting caprolactam to promote the ring-opening reaction. After refluxing the melt for another 30 min, TDI (0.6 wt% of the melting caprolactam) was added to the caprolactam. Thirdly, the melt was cast into the mold filled with GF cotton, Figure 2 (left and center), and the mold cavity was enclosed with a punch, Figure 2 (right). The caprolactam was polymerized for 20 min. The composite was then obtained and ejected from the mold. A composite plate prepared by this technology is shown in Figure 2 (bottom).

Cut from the composite plate, the specimen is shown in Figure 3 (right). The width ( $D$ ) and length of the specimen is respectively 50 mm and 80 mm, and the thickness of this plate is 1 mm, as shown in Figure 3 (left). The ends of the specimens act as gripped ends. The hole is drilled in the center of the specimens by a drilling machine. To investigate the effect of hole diameter on the SCF, the hole diameter is drilled as 2 mm, 3 mm, 4 mm, 5 mm, 6 mm, 7 mm, 8 mm, 9 mm, 10 mm, and 12 mm, respectively. All the holes are not drilled in different composite plates, but are successively drilled in the same plate. Therefore, the influence of the composite property on SCF may be avoided. Due to



**Figure 1.** GF cotton and nondirectional fibers. Left: GF cotton. Center: GF bundle. Right: GF in composite.

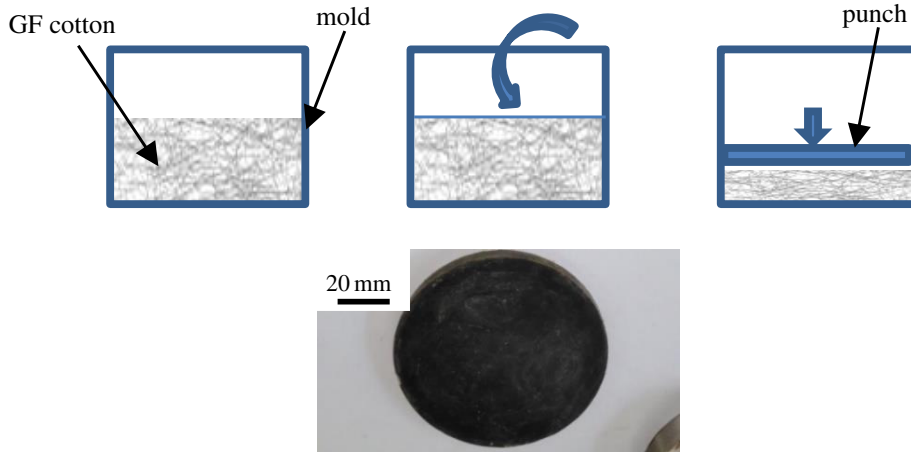


**Figure 2.** Preparation of GF cotton reinforced MC-nylon. Top: GF cotton in mold, pouring MC-nylon, and polymerizing. Bottom: GFCR MC-nylon plate.

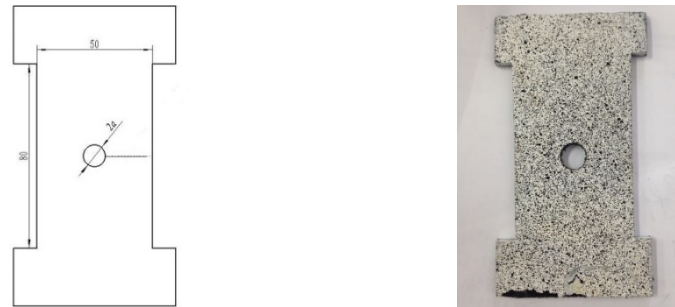


**Figure 3.** Experimental specimen. Left: specimen size (mm). Right: painted specimen.

the plate's thickness being 1 mm, and the fact that the minimum diameter of circular hole is 2 mm, the state of stress is approximately plane stress under simple tension conditions. Certainly, the state of stress is close to plane stress while the diameter of the circular hole increases. The DIC technique relies on contrasting patterns on the surface of the measured specimen. The color of the composite plate is black, therefore, the specimens should be painted with white and black paint subsequently, and this is shown in Figure 3 (center). The specimen preparation is as follows. Firstly, white paint is painted on the surface of the specimen. Then, tiny black paint-drops are evenly painted on the surface of the specimen. The maximum diameter of the black paint-drops is less than 0.2 mm.

In general, the SCF of a circular hole in an infinite plate is different from that in a finite plate. In other words, SCF is influenced by the ratio of plate width to circular hole diameter ( $D/2a$ ). However, for an isotropic plate, the research reveals that the finite plate can be viewed as an infinite plate on the condition that  $D/2a$  is more than 4 [Tan 1988]. In this study, the minimum  $D/2a$  of the specimen is 4.16. Therefore, the specimen with a circular hole can be viewed as an infinite plate and it is not necessary to take the effect of  $D/2a$  on SCF into account.

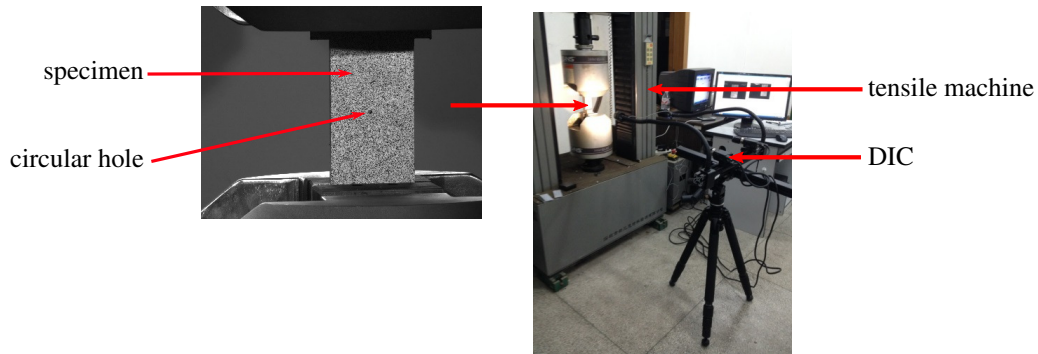


**Figure 4.** Experimental equipment.

### 3. Experimental equipment and procedure

DIC has been applied in many industrial areas, such as the automobile and aviation industries. DIC uses video cameras to record images on the surface of the testing specimen, stores them in digital form, and performs image analysis to extract the full-field shape, deformation, and motion measurements with the help of many types of object-based patterns, including lines, grids, dots, and random arrays. In this work, the authors use DIC to measure the strain field of a composite plate. The DIC system used in this investigation is named noncontacting full-field strain measurement system-VIC3D, which is manufactured by Correlated Solutions Inc. of the United States. The measuring length range of this DIC system is from 0.8 mm to 50 m, and the measuring strain range is from 0.001 to 20.

The DIC equipment and the specimens are shown in Figure 4. The composite specimen is clamped in the clamping chuck of the testing machine. The aim of this article is to investigate the SCF of the composite plate under elastic conditions. Therefore, the maximum stress loaded on the specimen is no more than 15 MPa, which is much less than the yield stress of 80 MPa for this composite. Moreover, the tensile loading applied to the specimen is adjusted according to the diameter of circular hole to ensure that the maximum stress in all experiments is identical. In this experiment, the frequency of taking pictures for DIC is set as 120 pictures per minute and the loading rate is set as 40 N/s, which indicates that loading is nearly quasistatic.

### 4. Experimental results and discussion

**4.1. Effect of diameter of circular hole on SCF.** A strain nephogram indicates the value of strain by color. Two strain nephograms of the composite specimen are shown in Figure 5, in which the strain along the loading direction  $\varepsilon_y$  is indicated by a different color. The maximum and minimum strains are displayed in red and burgundy, respectively. It can be seen from Figure 5 (left) that the strain of the specimen has approximate bilateral symmetry in space. Both the right and left sides of the circular hole in the strain nephogram are colored by red, especially near the edge of hole, which indicates that the deformation concentration is high in this area. In other words, the stress concentration first emerges near the edge of circular hole, while the strain concentration gradually disappears far away from the edge of hole. To evaluate the stress concentration of the circular hole, the strain values are extracted along the

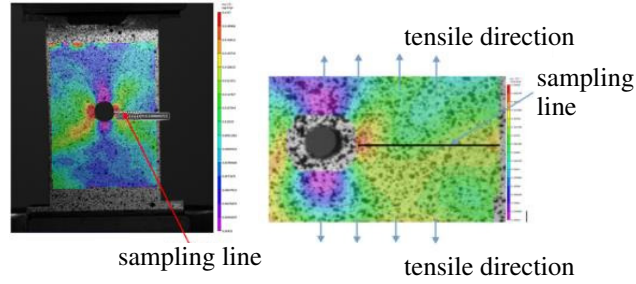


**Figure 5.** Strain nephogram around hole. Left: strain nephogram. Right: local strain nephogram.

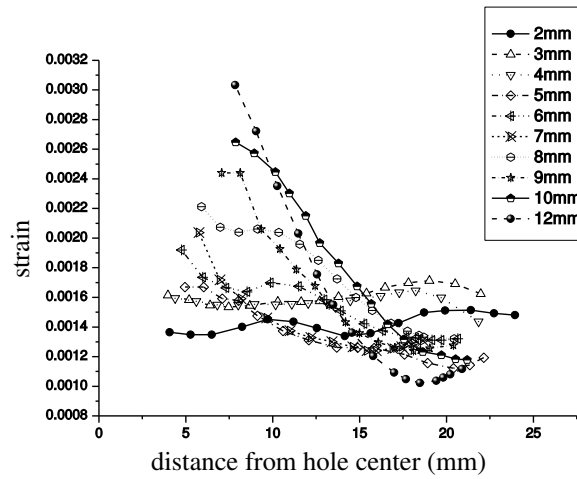


**Figure 6.** Strain distribution around circular hole.

horizontal sampling line shown in Figure 5, and are listed in Figure 6, in which the  $x$ -axis represents the distance from the central point to the sampling point and the  $y$ -axis indicates the corresponding strain. Intuitively, the fluctuation of strain curves is small when the diameter of the circular hole is less than 4 mm. In other words, the strain along the sampling line is almost even and the stress concentration is inapparent in this case. As the diameter of the whole increases, the strain near the hole edge increases, which leads to the slope of the strain curve to increase. Therefore, the stress concentration becomes more and more obvious.

Hole-edge stress concentration may be represented by SCF, which is the maximum stress of the hole edge divided by the average stress. For isotropic metal materials, the tangential direction tensile-stress distribution around the hole edge may be represented by

$$\sigma_{\rho}^m = \frac{\sigma^0}{2} \left( 1 + A \frac{a^2}{\rho^2} + \left( 1 + B \left( \frac{4a^2}{\rho^2} - \frac{3a^4}{\rho^4} \right) \right) \cos 2\varphi \right), \quad (1)$$

where  $\sigma_{\rho}^m$  represents the tangential direction tensile-stress,  $\sigma^0$  stands for the nominal stress,  $a$  is the radius of the circular hole,  $\rho$  represents the distance from the measured point to the center of the hole, and  $\varphi$  is the deviation angle from tensile direction. In (1),  $\sigma_{\rho}^m$  reaches its maximum value when  $\varphi$  is  $90^{\circ}$ .



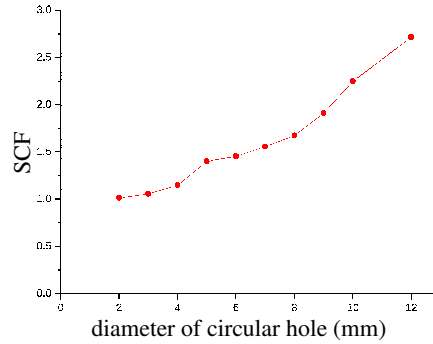


**Figure 7.** Experimental SCF of the composite.

In (1),  $A$  and  $B$  are determined by

$$A = \frac{(1 - v^m - 2(v^m)^2)E^f - (1 - v^f - 2(v^f)^2)E^m}{E^f(1 + v^m) + E^m(1 - v^f - 2(v^f)^2)}, \quad (2)$$

$$B = \frac{E^m(1 + v^f) - E^f(1 + v^m)}{-E^m(1 + v^f) + E^f(-3 + v^m + 4(v^m)^2)}, \quad (3)$$

in which  $E^m$  and  $E^f$  are respectively the elastic modulus of the resin and the fiber, and  $v^m$  and  $v^f$  are the volume fraction of the resin and the fiber, respectively. Therefore, (1) shows that the SCF is not only determined by the constituent original properties, but also by the composite geometric parameters such as the fiber volume fraction.

For the GF cotton reinforced MC-nylon,  $E^m$  and  $E^f$  are 3 GPa and 80 GPa respectively;  $v^m$  and  $v^f$  are 0.85 and 0.15 respectively. Therefore, while  $a$  is equal to  $\rho$ , the maximum SCF calculated from (1) is about 1.9.

In this paper, we define the maximum SCF for the composite just as in an isotropic plate; namely, as the maximum stress of the hole edge divided by the average stress. Then we calculate the maximum SCF of the composite from Figure 6 and list the SCF in Figure 7, which shows that the maximum SCF of the composite increases as the diameter of the circular hole increases. The maximum SCF is between 1.012 and 2.726, which is different from 1.9, as calculated by (1). Therefore, the experimental results show that (1) is not suitable for calculating the SCF of this composite. This may be caused by the influence of the diameter of circular hole and the length of GF.

As shown in Figure 1 and Figure 8 (left), the GF in this composite is bent and tangled up, which constitutes a fiber network. Under tension stress, the GF around the circular hole acts as “rebar”. The GF network reinforces the matrix and transmits the strain far away from the hole edge. Compared to the stiffness of matrix, the stiffness of GF is higher. Therefore, the GF network in the composite acts as “anchoring” and “tangling”, which alleviates the strain concentration near the hole edge and decreases the SCF. Moreover, the experimental results show that the maximum SCF of this composite is more than that calculated by (1).

Unidirectional fiber-reinforced composites have been widely applied in industries, and its maximum SCF of a circular hole may be much more than that in the isotropic case. For example, the maximum SCF of a typical unidirectional carbon-fiber-reinforced composite is 9.37 [Liu and Tang 2016], which

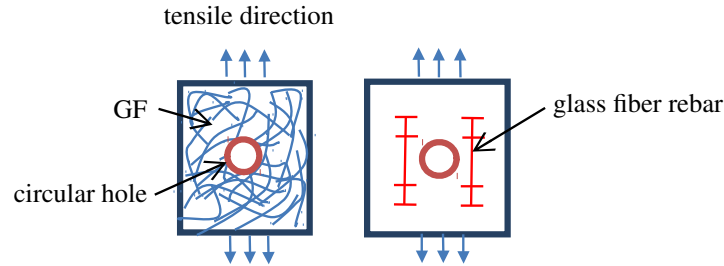


**Figure 8.** Anchoring (left) and tangling (right) of fiber network.

indicates that the stress concentrates around the hole edge seriously. Although the length and strength of the carbon fiber in [Liu and Huang 2014] is much higher than that of the GF in this composite, the SCF of the carbon-fiber-reinforced composite is much higher than that of this composite. The cause may lie in that the unidirectional fiber in composite can be viewed as “round steel” and the fibers network in composite act as rebar. It is evident that the anchoring and tangling of the fiber network alleviate the stress concentration. Therefore, the conclusion may be drawn that the length and strength of the fiber is not the sole factor in influencing the SCF of circular hole. Sometimes the distribution of fibers plays a more important role in alleviating stress concentration.

Figure 8 indicates that the maximum SCF of the composite is determined by hole size and microstructure size. On the one hand, the bigger the hole, the higher the SCF. For example, when the diameter is 2 mm, the corresponding SCF is close to 1, and the maximum SCF is 2.726 when the diameter is 12 mm. All experimental results are obtained from the same specimen and the center of all the circular holes are identical. Therefore, the influence of the material properties on the SCF can be excluded. The factors that affect the SCF are hole size and microstructure size. Microstructure size, namely the average GF length around the hole, also influences the SCF. A sketch of the distribution of GFs and the circular hole are shown in Figure 9. The length of all GFs are identical and the orientation of GFs is random. The average length of fibers around the circular hole is determined by the diameter of the circular hole. The authors developed a program to calculate the average length of the GFs around the hole, which is shown in Figure 10. It can be found from Figure 10 that the larger the diameter, the smaller the average length of GF. While the diameter of hole is 12 mm, the average length of the GF decreases from 60 mm to 55 mm. The average length of GF is approximately negative linear with the diameter of circular hole.

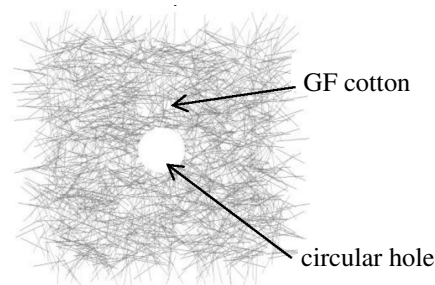


**Figure 9.** Circular hole and random distribution of GFs.

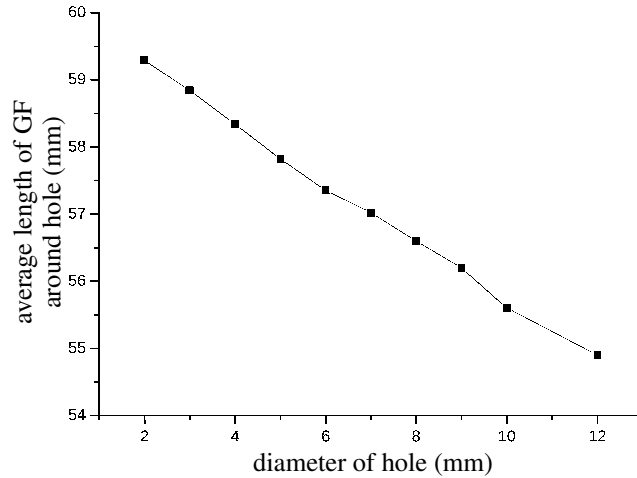


**Figure 10.** The average length of fibers around the circular hole.

As the average length of the GFs reduce, the effect of anchoring and tangling weakens. Therefore, the stress concentrates near the hole edge and the SCF increases. Moreover, the integrity of the GF network weakens as the diameter of the circular hole increases. In a word, the integrity of the GF network and the average length of the GF around circular hole influence the SCF, and the SCF of the composite is determined by hole size and GF size.

**4.2. Effect of stress intensity on SCF.** Generally, SCF is unrelated to the stress  $\sigma^0$ , as shown in (1). However, the experimental results show that the SCF of this composite is related to the stress  $\sigma^0$ . With the help of the DIC system, the authors recorded the strain around circular hole under different stress intensities (3 MPa, 5.5 MPa, 8 MPa, and 10 MPa). The SCF under different stress intensities and different diameters of the circular hole is shown in Figure 11. On the whole, for all circular holes, the higher the stress, the lesser the SCF. For example, the SCF of the 10 mm circular hole decreased from 2.92 to 2.34 (about 20%), while the stress increased from 3 MPa to 10 MPa.

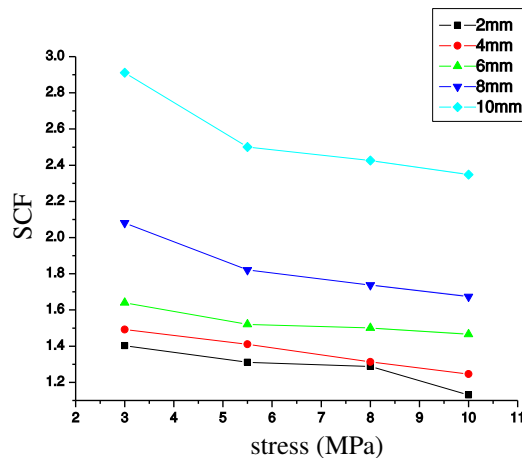


**Figure 11.** SCF under different nominal stresses.

In our knowledge, the SCF of the circular hole edge is unrelated to the nominal stress under static loads for isotropic composites. The authors advocate that both the material construction of the composite and the distribution of the GF influence the SCF under static load. As opposed to a single phase material such as metal, the composite consists of two phases: the matrix phase MC-nylon and the reinforced phase GF. The mechanical properties of the reinforcing material GF is much different from that of MC-nylon. For example, the modulus of elasticity of MC-nylon is about 3 GPa, which is much less than that of GF, which is 80 GPa. Therefore, under the same stress, the deformation of the soft matrix phase is much larger than that of rigid GF. Under the action of axial loading, the MC-nylon around the bilateral of the circular hole deforms first, and then the stress is transmitted to the reinforced phase. At the same time, the reinforced phase works faintly under low stress intensity. In other words, the concentrated strain of the matrix around the hole edge is hardly transmitted from the hole edge. Therefore, the strain concentrates around the hole edge and the SCF is high. When the nominal stress increases, the reinforced phase works and the strain concentration around the hole edge weakens, which leads to a decrease of SCF.

Also, Figure 11 shows that the reduction of SCF varies with the diameter of the hole. The reduction ratios of the SCF for 2 mm, 4 mm, 6 mm, and 8 mm circular holes are 19.2%, 16.8%, 14.9%, 19.7%, respectively. The average GF length and the integrality of GF network around the circular hole may play an important role in the reduction of the SCF. The smaller the diameter of circular hole, the longer the average GF length and the better the integrality of the GF network. In other words, the reinforced phase works effectively regardless of the nominal stress. Therefore, the SCF of the 2 mm circular hole is the minimum regardless the stress intensity.

## 5. Finite element analysis

**5.1. Finite element model.** The reason why the commercial FEM code is not suited to analyze the influence of the length and proportion of the fibers on stress concentration is illustrated in Section 1. It is necessary to suggest a novel method to simulate the stress concentration of a circular hole for this composite. The core idea of this simulation model is that the matrix phase and reinforced phase in this composite are assigned different material properties respectively. Moreover, the GF is simplified as a bar and its distribution is random. In this composite, the diameter of the GF is 13 microns and the number of GFs is massive, which may lead to the number of elements in the simulation model being extremely massive. Therefore, the authors simplify the GF as a bar with a square cross section. The side length of the square cross section is 0.8 mm, and the length of the bar is identical to the GF length. It is noted that the volume fraction of the GF in this simulation model is identical to that of the 21% composite. In this FEM model, the Solid185-type element is applied to mesh the MC-nylon and the GF. First, the GF is meshed with the element size 0.4 mm. Then the MC-nylon is meshed with the adaptive element, and the interface elements between the MC-nylon and GF are coincided.

The geometric modeling is as follows. The first step is to construct the geometric model of GF through the loop statement in the APDL language. The GF bars are confined within a cuboid. Length, width, and thickness of the cuboid are respectively 80 mm, 50 mm, and 5 mm, which is identical to the dimensions of the specimen. The distribution of the GF is random and uniform in the matrix. To investigate the influence of GF length on the SCF, the GF length are 13 mm, 26 mm, 38 mm, and 60 mm, respectively. For example, the GF length in Figure 13 is 13 mm. The number of GF bars depends on the volume of

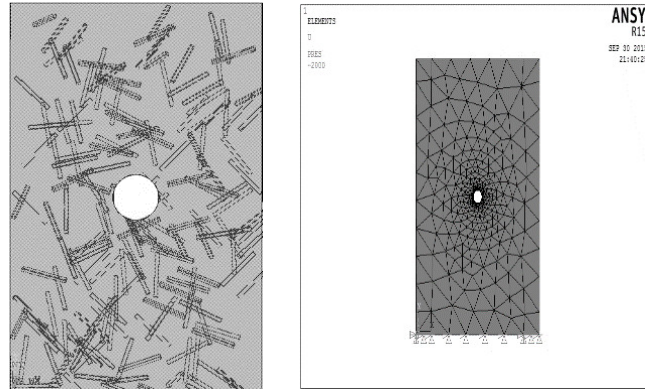


**Figure 12.** The geometric model (left) and finite element model (right).

a single GF bar and the volume fraction of the GF in the composite. The second step is to construct the geometric model of the matrix, and the volume of GF bars is removed from the cuboid by Boolean operation. It is noted that the dimension of the cuboid is the same as that of the specimen, and the diameter of the circular hole varies from 2 mm to 12 mm. Figure 12 (left) shows this model and the random distribution of GFs.

The matrix and GF are meshed sequentially by the element type Solid185. The element size for the GF is 0.4 mm. Then the matrix elements and the GF elements are combined with the linkage of nodes, shown in Figure 12 (right). The bottom edge of the model is fixed, and a load of 2000 N is applied to the upper side nodes. The boundary condition and load applied on the finite model is identical to that in the experiment.

**5.2. Results and discussion.** The simulation results obtained from the above simulation model are shown in Figure 13. Firstly, the simulated SCF and the experimental SCF are compared when the GF length is

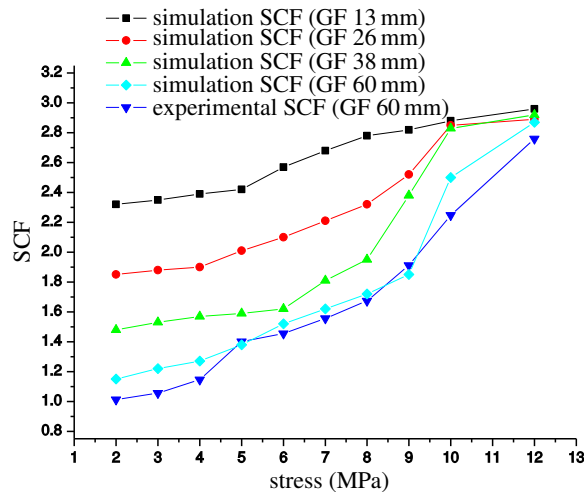


**Figure 13.** Simulation results.



60 mm. Although the former value is a bit more than the latter one as a whole, the average difference between the two SCFs is only 5.6%. Therefore, it is consistent between the experimental SCF and the simulation results. Figure 13 also shows that the shorter the GF in the composite, the larger the SCF. The average SCF for the composite with 38 mm, 26 mm, and 13 mm long GFs is 1.97, 2.25, and 2.62 respectively. Moreover, Figure 13 indicates that the gradient of SCF curves decreases as the GF shortens. For example, when the GF length is 13 mm, the SCF increases from 2.32 to 2.96 and the corresponding variation of the SCF is 21.6%. For 60 mm GF, the SCF raises from 1.14 to 2.76 and the corresponding variation of the SCF reaches 58.6%. It may be that the “anchoring” and “tangling” of the fiber network weakens as the GF shortens, and the strain concentrates around the edge of circular hole. Moreover, it can be easily seen that the SCF is close to 3 while the diameter of circular hole is 12 mm regardless of GF length. This may be induced by the decrease in the average length of the GF and the weakening of anchoring and tangling, which has been discussed in Section 2.

For the isotropic plate without fiber reinforcement, the SCF of the circular hole is 3 and is unrelated to the diameter of the circular hole. In other words, the corresponding SCF curve is a horizontal line because there is no anchoring or tangling of fiber network. When the GF length in this composite is close to zero, the composite is similar to the isotropic plate without fiber reinforcement. It is obvious that the simulation results shown in Figure 13 are rational. Therefore, the SCF of the circular hole of the composite is related to both the diameter of the circular hole and the GF length.

## 6. Conclusion

In this paper, a novel composite named as glass-fiber-cotton reinforced MC-nylon is prepared and the stress concentration of a circular hole of this composite is investigated with the digital image correlation technique. The experimental results show that the maximum SCF of the composite increases as the diameter of circular hole increases. Also, the higher the stress intensity, the lesser the SCF. Moreover, a novel simulation model to investigate the SCF of this material is suggested, showing that the shorter the GF in composite, the larger the SCF. In a word, the SCF of this composite is influenced by the GF length, the stress intensity, and the diameter of the circular hole.

## Acknowledgments

This work is supported by the National Natural Science Foundation of China (Grant No. 51675173), National key R&D Program of China (Grant No. 2017YFB1301300), and State Key Laboratory of Reliability and Intelligentization for Electrical Equipment of China (Grant No. EERIZZ2018001).

## References

- [Aparna et al. 2015] M. L. Aparna, G. Chaitanya, K. Srinivas, and J. A. Rao, “Fatigue testing of continuous GFRP composites using digital image correlation (DIC) technique a review”, *Materials Today: Proceedings* 2:4-5 (2015), 3125–3131.
- [Bao and Liu 2016] H. Bao and G. Liu, “Progressive failure analysis on scaled open-hole tensile composite laminates”, *Compos. Struct.* **150** (2016), 173–180.
- [Cheng and Chen 1988] S. Cheng and D. Chen, “On the stress distribution in laminae”, *J. Reinf. Plast. Compos.* **7**:2 (1988), 136–144.
- [Ghasemi and Razavian 2012] A. R. Ghasemi and I. Razavian, “Measurement of variation in fracture strength and calculation of stress concentration factor in composite laminates with circular hole”, *J. Solid Mech.* **4**:3 (2012), 226–236.

- [Hao et al. 2015] A. Hao, L. Yuan, and J. Chen, “Notch effects and crack propagation analysis on kenaf/polypropylene nonwoven composites”, *Compos. A Appl. Sci. Manuf.* **74** (2015), 11–19.
- [Jadee and Othman 2015] K. Jadee and A. R. Othman, “Analysis of stress mitigation through defence hole system in GFRP composite bolted joint”, *Am. J. Mech. Eng.* **3:4** (2015), 126–134.
- [Khoroshun and Kabysh 2007] L. P. Khoroshun and Y. M. Kabysh, “Gradient model in the problem of stress-concentration around a circular hole in two-component stochastic composites”, *Int. Appl. Mech.* **43:12** (2007), 1336–1346.
- [Lekhnitskii et al. 1968] S. G. Lekhnitskii, W. S. Tsai, and T. Cheron, *Anisotropic plates*, Gordon and Breach Science Publishers, New York, 1968.
- [Liu and Huang 2014] L. Liu and Z. Huang, “Stress concentration factor in matrix of a composite reinforced with transversely isotropic fibers”, *J. Compos. Mater.* **48:1** (2014), 81–98.
- [Liu and Tang 2016] G. Liu and K. Tang, “Study on stress concentration in notched cross-ply laminates under tensile loading”, *J. Compos. Mater.* **50:3** (2016), 283–296.
- [Maximiyuk et al. 2014] V. A. Maximiyuk, E. A. Storozhuk, and I. S. Chernyshenko, “Stress state of flexible composite shells with reinforced holes”, *Int. Appl. Mech.* **50:5** (2014), 558–565.
- [Moure et al. 2016] M. M. Moure, S. K. García-Castillo, S. Sánchez-Sáez, E. Barbero, and E. J. Barbero, “Influence of ply cluster thickness and location on matrix cracking evolution in open-hole composite laminates”, *Compos. B Eng.* **95** (2016), 40–47.
- [Pandita et al. 2003] S. Pandita, K. Nishiyabu, and I. Verpoest, “Strain concentrations in woven fabric composites with holes”, *Compos. Struct.* **59:3** (2003), 361–368.
- [Paul and Rao 1995] T. K. Paul and K. M. Rao, “Finite element stress analysis of laminated composite plates containing two circular holes under transverse loading”, *Comput. Struct.* **54:4** (1995), 671–677.
- [Savruk and Kazberuk 2007] M. P. Savruk and A. Kazberuk, “A unified approach to problems of stress concentration near V-shaped notches with sharp and rounded tip”, *Int. Appl. Mech.* **43:2** (2007), 182–197.
- [Tan 1988] S. C. Tan, “Finite-width correction factors for anisotropic plate containing a central opening”, *Compos. Mater* **22** (1988), 1080–1097.
- [Toubal et al. 2005] L. Toubal, M. Karama, and B. Lorrain, “Stress concentration in a circular hole in composite plate”, *Compos. Struct.* **68:1** (2005), 31–36.
- [Wang et al. 2013] S. B. Wang, B. Teng, and S. Zhang, “Torsional wear behavior of monomer casting nylon composites reinforced with GF: effect of content of GF”, *Tribology Trans.* **56** (2013), 178–186.
- [Wu and Mu 2003] H.-C. Wu and B. Mu, “On stress concentrations for isotropic/orthotropic plates and cylinders with a circular hole”, *Compos. B Eng.* **34:2** (2003), 127–134.
- [Xu et al. 2013] S. Xu, X. Zhao, and L. Ye, “Mechanical and crystalline properties of monomer casting Nylon-6/SiO<sub>2</sub> composites prepared via in situ polymerization”, *Polym. Eng. Sci.* **53:9** (2013), 1809–1822.
- [Zhang et al. 2012] S. Zhang, C. Cui, and G. Chen, “Tribological behavior of MC Nylon6 composites filled with glass fiber and fly ash”, *J. Wuhan Univ. Technol.-Mat. Sci. Edit.* **27:2** (2012), 290–295.

Received 21 Jan 2018. Revised 5 May 2018. Accepted 10 May 2018.

YOU RUI TAO: taoyourui@hebut.edu.cn

State Key Laboratory of Reliability and Intelligence of Electrical Equipment, Hebei University of Technology, Tianjin, China

NING RUI LI: 316470923@qq.com

College of Mechanical Engineering, Hebei University of Technology, tianjin, China

XU HAN: xhan@hebut.edu.cn

College of Mechanical Engineering, Hebei University of Technology, Tianjin, China



# JOURNAL OF MECHANICS OF MATERIALS AND STRUCTURES

msp.org/jomms

Founded by Charles R. Steele and Marie-Louise Steele

## EDITORIAL BOARD

ADAIR R. AGUIAR	University of São Paulo at São Carlos, Brazil
KATIA BERTOLDI	Harvard University, USA
DAVIDE BIGONI	University of Trento, Italy
MAENGHYO CHO	Seoul National University, Korea
HUILING DUAN	Beijing University
YIBIN FU	Keele University, UK
IWONA JASIUKEWICZ	University of Illinois at Urbana-Champaign, USA
DENNIS KOCHMANN	ETH Zurich
MITSUTOSHI KURODA	Yamagata University, Japan
CHEE W. LIM	City University of Hong Kong
ZISHUN LIU	Xi'an Jiaotong University, China
THOMAS J. PENCE	Michigan State University, USA
GIANNI ROYER-CARFAGNI	Università degli studi di Parma, Italy
DAVID STEIGMANN	University of California at Berkeley, USA
PAUL STEINMANN	Friedrich-Alexander-Universität Erlangen-Nürnberg, Germany
KENJIRO TERADA	Tohoku University, Japan

## ADVISORY BOARD

J. P. CARTER	University of Sydney, Australia
D. H. HODGES	Georgia Institute of Technology, USA
J. HUTCHINSON	Harvard University, USA
D. PAMPLONA	Universidade Católica do Rio de Janeiro, Brazil
M. B. RUBIN	Technion, Haifa, Israel

**PRODUCTION** production@msp.org

SILVIO LEVY Scientific Editor

---

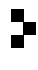
See [msp.org/jomms](http://msp.org/jomms) for submission guidelines.

JoMMS (ISSN 1559-3959) at Mathematical Sciences Publishers, 798 Evans Hall #6840, c/o University of California, Berkeley, CA 94720-3840, is published in 10 issues a year. The subscription price for 2018 is US \$615/year for the electronic version, and \$775/year (+\$60, if shipping outside the US) for print and electronic. Subscriptions, requests for back issues, and changes of address should be sent to MSP.

---

JoMMS peer-review and production is managed by EditFLOW<sup>®</sup> from Mathematical Sciences Publishers.

PUBLISHED BY

 **mathematical sciences publishers**  
nonprofit scientific publishing

<http://msp.org/>

© 2018 Mathematical Sciences Publishers

# Journal of Mechanics of Materials and Structures

Volume 13, No. 3

May 2018

- 
- Formulas for the H/V ratio of Rayleigh waves in compressible prestressed hyperelastic half-spaces** PHAM CHI VINH, THANH TUAN TRAN, VU THI NGOC ANH and LE THI HUE 247
- Geometrical nonlinear dynamic analysis of tensegrity systems via the corotational formulation** XIAODONG FENG 263
- Shaft-hub press fit subjected to couples and radial forces: analytical evaluation of the shaft-hub detachment loading** ENRICO BERTOCCHI, LUCA LANZONI, SARA MANTOVANI, ENRICO RADI and ANTONIO STROZZI 283
- Approximate analysis of surface wave-structure interaction** NIHAL EGE, BARIŞ ERBAŞ, JULIUS KAPLUNOV and PETER WOOTTON 297
- Tuning stress concentrations through embedded functionally graded shells** XIAOBAO LI, YIWEI HUA, CHENYI ZHENG and CHANGWEN MI 311
- Circular-hole stress concentration analysis on glass-fiber-cotton reinforced MC-nylon** YOU RUI TAO, NING RUI LI and XU HAN 337
- Elastic moduli of boron nitride nanotubes based on finite element method** HOSSEIN HEMMATIAN, MOHAMMAD REZA ZAMANI and JAFAR ESKANDARI JAM 351
- Effect of interconnect linewidth on the evolution of intragranular microcracks due to surface diffusion in a gradient stress field and an electric field** LINYONG ZHOU, PEIZHEN HUANG and QIANG CHENG 365
- Uncertainty quantification and sensitivity analysis of material parameters in crystal plasticity finite element models** MIKHAIL KHADYKO, JACOB STURDY, STEPHANE DUMOULIN, LEIF RUNE HELLEVIK and ODD STURE HOPPERSTAD 379
- Interaction of shear cracks in microstructured materials modeled by couple-stress elasticity** PANOS A. GOURGIOTIS 401



1559-3959(2018)13:3;1-Z